

Kalman Filter-Driven Blind Source Localization for Passive 3D ToF Imaging

Faisal Ahmed^{1*}, Miguel Heredia Conde^{1,2}, and Paula López Martínez²

¹Center for Sensor Systems (ZESS), University of Siegen, Germany

²CITIUS, Universidade de Santiago de Compostela, Spain

Manuscript received June 7, 2017; revised June 21, 2017; accepted July 6, 2017. Date of publication July 12, 2017; date of current version July 12, 2017.

Abstract—Passive 3D Time-of-Flight (ToF) imaging faces a significant challenge in accurate depth recovery, where the source position is unavailable. In this letter, we present a probabilistic approach based on the Kalman filter which keeps track of source location, thus, avoiding the need for an initial guess to jointly determine the 3D source position and correct depth information. The proposed approach is able to reach a source location error of 0.8 cm by exploiting pseudo-measurements of the plane fitting constraint acquired by a passive ToF camera which exploits a bistatic algorithm with a gradient descent method. Computer experiments are carried out to demonstrate the robustness of the proposed method in realistic scenarios where no initial guess is available. The results show the feasibility of blind source localization with mm accuracy. This contributes to widening the applicability of passive 3D imaging in a number of application fields, such as autonomous driving, and robot navigation.

Index Terms—Blind source localization, Passive imaging, Depth reconstruction, sensor signal processing, Kalman filter.

I. INTRODUCTION

Blind 3D source localization has emerged as a fundamental requirement for many tasks such as passive imaging, where its appearance has been promoted by advancements in lighting infrastructure, which can potentially be exploited as an opportunity illuminator [1], wireless communication for better resource allocation [2], indoor positioning [3] and robot navigation [4]–[6], and Internet-of-Things (IoT) [7]. Despite recent activity around the topic, the source location remains an open question for passive imaging and resource allocation for wireless communication from both a theoretical and practical perspective.

Driven by the idea of simultaneous communication and sensing (SCAS) [8], [9], we consider blind source localization as a key sensing task that is drawn from legacy optical wireless communication [10]. Fortunately, this idea aligns with the underlying principles of passive ToF imaging, which uses visible light communication (VLC) sources as *opportunity illuminators*. Therefore, our aim is to introduce blind source localization by leveraging a geometry-inspired bistatic setting and reusing optical signals to achieve the objectives of both 3D sensing and source localization. This would be a relevant step towards *joint sensing and localization* (JSAL), which can be attained by combining sensing and passive localization operations based on bistatic principles. In passive ToF, the existence of one direct and one indirect sensing path yields a bistatic configuration [11]. [12] has studied the ellipsoidal localization problem when the source location is unknown. A large body of work assumes that the source position is known [13]–[15]. However, relying on a known source location is not a realistic assumption in general.

To address the 3D ellipsoid localization problem, an iterative probabilistic approach is developed in this work to jointly estimate the source position and correct depth information. We make use of a Kalman filter (KF) to keep track of the source location over

time, thus enhancing the robustness of our estimation procedure and attaining a correct depth estimate in a limited number of iterations. Differently from the existing works, we use an intuitive tactic for solving such a localization problem without knowing the source position that leverages a planarity constraint combining plane-fitting with gradient descent optimization in the art of a plug-and-play (PnP) algorithm. The KF allows for keeping track of the variance of the 3D location estimate in real time and optimally incorporating new measurements to the predicted state. We use optimization procedure in [12] to get pseudo-measurements, which we then use as a proxy measurement of source position in a Kalman-driven process. A number of computer simulations are carried out using fixed receiver positions and constant velocity under realistic frame rate assumptions to demonstrate the feasibility of our proposed method.

II. THE LOCALIZATION METHODOLOGY

The 3D ellipsoid localization problem is considered in this work, which is an extension of [12], where a single source and two co-located receivers are exploited to jointly estimate the position of an unknown source and correct the depth estimates. The unknown 3D source initial position and velocity are denoted by $P_E^o \in \mathbb{R}^3$ and $V_E^o \in \mathbb{R}^3$, respectively. The co-located receivers are at a known position, $P_R \in \mathbb{R}^3$, and synchronized externally. In passive ToF, one receiver is a photodetector that acquires the reference signal for synchronization, while the other is actually an array of ToF pixels that capture the echoes from the scene. The receiver not only observes the reflected signal from the target but also receives the direct signal from the emitter.

We exploit a gradient descent scheme for solving blind source localization problem [12]. In each iteration of bistatic passive gradient descent (BP-GD), we displace the source location to enhance the assumed local planarity. In this work, we develop a more practical method of probabilistic approach that leverages the power of the KF to accelerate blind source localization and avoid the need for an accurate initialization at each new data acquisition.

However, no real measurements of the source location are available to update the KF estimate. In this setting, one plausible approach

Corresponding author: Faisal Ahmed (e-mail: Faisal.Ahmed@uni-siegen.de).

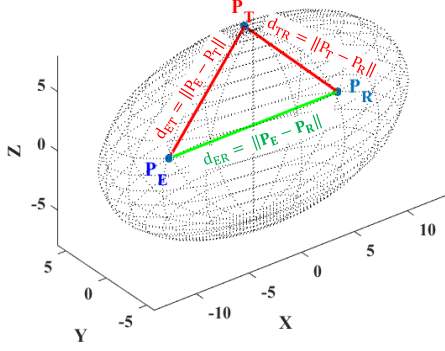


Fig. 1. Joint source localization and depth recovery bistatic setup.

is to attain a pseudo-measurement from a plane fitting constraint, instead of an additional sensor for obtaining the 3D source position measurements, by considering that most targets exhibit local planarity. The most common case in practice is the *Manhattan world* (vertical planarity) assumption, which has been demonstrated as having potential for the 3D reconstruction task, as reported in [16].

A. Ellipsoid Localization Scenario

A bistatic configuration is composed of a single emitter and two co-located receivers, yielding the ellipsoid localization constraint demonstrated in Fig. 1. An emitter emits an optical waveform, which is bounced back by the target and then received by the ToF sensor; this propagation channel is generally known as an indirect channel in the literature [1], [8]. A direct channel is established between the emitter and reference photodiode separated by a direct distance. Thanks to lens calibration, 3D target points can be obtained by the intersection of the ellipsoid and the direction vectors. The emitter position may be unavailable in such settings. In this work, we aim to combine KF tracking with GD optimization to jointly estimate the source position and target 3D depth reconstruction. The 3D target location can be formulated as follows:

$$P_T = P_R + \vec{n}_R d_{RT} \quad (1)$$

where P_T and P_R are 3D target and receiver points and \vec{n}_R is the unit vector along observation direction, and d_{RT} is the distance between the receiver and the target. The bistatic range is the difference between the emitter-target-ToF sensor and emitter-receiver distances. The locus of constant bistatic range defines a 3D ellipsoid, where emitter and receiver positions are serving as its foci as shown in Fig. 1, can be defined by,

$$d = d_{ET} + d_{RT} - d_{ER} \quad (2)$$

A previous version of the derivation, supposing a known source location and eliminating the effect of d_{ER} by calibration, can be found in [1]. The total distance is demonstrated by d , here termed as *incorrect depth*. $d_{ET} = \|P_E - P_T\|_2$ is the Euclidean distance between the emitter and the target. Equation (2) is rearranged and we reformulate (1) into 3D coordinate components and plug it into (2) for further derivation. For brevity, the complete derivation has been omitted.

In this work, the bistatic algorithm additionally accounts for the effect of the direct distance, d_{ER} . The corrected depth, $d_{RT} = f_{d_{RT}}(d, P_E)$,

is a function of the *incorrect depth* d and the 3D position of an emitter, P_E , as follows,

$$f_{d_{RT}}(d, P_E) = \frac{d^2 + 2dd_{ER}}{2d + 2d_{ER} - 2G} \quad (3)$$

where $d_{ER} = \|P_E - P_R\|_2$ and G is the $\langle (P_E - P_R), \vec{n}_R \rangle$. If P_E was known a priori, (3) provides the correct distance to the target. In this work, we aim to retrieve the latter for an uncertain P_E .

B. Pseudo Measurements

We consider a ToF camera operated in externally triggered pulsed mode, more specifically we use a ToF camera based on the *photonic mixer device* (PMD) in our experiments. The resultant system emulates a cross-correlation between emitted and reflected signals in the optical domain [17]. Our attention is limited to a planar region whose points follow equation (4). The 3D plane points, $\{P_i\}_{i=1}^N$, are generated by exploiting the camera lens normals for the N pixels in simulations. To generate measurements synthetically, the known emitter and receiver positions are used as our ground truth (GT), and an incorrect depth estimate is computed from the camera measurements (more details can be found in [12]). A plane can be defined as:

$$Z = aX + bY + c \quad (4)$$

where $\vec{x} = (a, b, c)$ represents a normal vector and $Z = [z_1, z_2, \dots, z_N]^T$, $X = [x_1, x_2, \dots, x_N]^T$, and $Y = [y_1, y_2, \dots, y_N]^T$ are the 3D plane points. The plane points are given by the number of pixels in the array denoted by N . This can be formulated as a linear system of equations $\mathbf{A}\vec{x} = Z$ and is treated as an inverse problem involving the recovery of the unknown plane parameter, \vec{x} . The matrix \mathbf{A} is formed as $\mathbf{A} = [X, Y, O]$, where $O = [1, 1, \dots, 1]^T$, and $\mathbf{A} \in \mathbb{R}^{N \times 3}$. This plane fitting problem becomes an overdetermined system, as $N \gg 3$, and the normal vector \vec{x} can be estimated from Z by the Moore-Penrose pseudoinverse $\mathbf{A}^\dagger = (\mathbf{A}^T \mathbf{A})^{-1} \mathbf{A}^T$. The least squares (LS) solution of the system is $\hat{\vec{x}}$ and we obtain fitted plane points by plugging in (4).

With the concept of pseudo-measurements, this approach lays the groundwork to treat the ellipsoidal problem to recover the source position and correct depth information. ToF measurements are used to compute the depth using (2), which is known as an incorrect depth. This depth is plugged into the bistatic algorithm (3) to obtain the correct depth estimates. In this case, we attempted to solve the unknown source position problem by exploiting the plane fitting with the least squares solution. The distance between each corrected depth and the corresponding point in fitted plane defines a cost function (5), $C(f_{d_{RT}}(d, P_E), d_{Fit})$, that is continuous on P_E . The cost function is formulated as follows,

$$C(f_{d_{RT}}(d, P_E), d_{Fit}) = \frac{1}{N} \sum_{n=1}^N (f_{d_{RT}}(d, P_E) - d_{Fit})^2 \quad (5)$$

where d_{Fit} represents the distance to each point in the fitted plane (4). Gradient descent is applied using the gradient of the cost function with respect to the 3D components of the emitter position. The gradient involves computing partial derivatives of the cost function w.r.t the corresponding 3D coordinate components. A gradient descent step generates pseudo-measurements of the source position. Y_p defines the pseudo-measurements, which can be written as,

$$Y_p := P_E \leftarrow P_E - \eta \frac{\partial C(P_E)}{\partial P_E} \quad (6)$$

where η is the step size.

C. Localization Algorithm Setting using Kalman Filter

A KF is rooted in statistical estimation techniques and is known to be an optimal linear estimator [18] under the assumptions of a linear system model and white Gaussian noise. Building upon the wide application of KFs in tracking applications [19], [20], we exploit it for obtaining accurate source position and depth information.

Our main goal is to enhance the robustness of the emitter position estimation. Following the KF structure, our approach consists of two stages: prediction and update states. To implement the KF process into the bistatic framework, we solve the pseudo-measurements problem (i.e., emitter position) by the method in [12] as summarized in algorithm 1. Below, we enumerate the iterative steps for simultaneous emitter position estimation and depth reconstruction.

- 1) Given the incorrectly measured depth d , we compute the correct depth in (3) by exploiting emitter position predicted via KF. For the update step, we leverage pseudo-measurements obtained from (6). The cost is a function of the corrected and fitted plane depth, d_{Fit} . The fitted plane depth is computed via steps 10 to 11. A gradient descent step yields the next pseudo-measurement in an iterative procedure.
- 2) We update the emitter position using the pseudo-measurements and pre-computed co-variances. Each emitter position update is given by the projection of innovation (line 18) given by the measurements through Kalman gain.

Algorithm 1 Kalman Filter-driven Blind Source Localization using Bistatic Algorithm with Gradient Descent

```

1: Inputs:  $\eta, P_E^o, P_R, \vec{n}_R, d^{(k)}, \bar{X}^o, \bar{P}^o$ 
2: Result:  $\bar{P}_E^{(K)}, C(P_E^{(K)}), d_{\text{RT}}^{(K)}$ 
3: for  $k \leftarrow 1$  to  $K$  do
4:   Prediction:
5:   Propagate state:  $\bar{X}^{(k)} = \mathbf{F}\bar{X}^{(k-1)} + \mathbf{W}^{(k)}$ 
6:   Propagate covariance:  $\bar{P}^{(k)} = \mathbf{F}\bar{P}^{(k-1)}\mathbf{F}^T + \mathbf{Q}^{(k)}$ 
7:   for  $j \leftarrow 1$  to  $J$  do
8:     Measurement update:
9:     Compute corrected depth:  $d_{\text{RT}}^{(j)}$  using (3)
10:    Construct matrix  $\mathbf{A}$  and Estimate:  $\hat{x}^j = \mathbf{A}^{\dagger j} \mathbf{Z}^j$ 
11:    Updated plane fitting model:  $d_{\text{Fit}}^{(j)}$  using (4)
12:    Update the cost function:
13:     $C(P_E^{(j-1)}) := \frac{1}{N} \sum_{n=1}^N (f_{\text{drt}}(d^{(k)}, P_E^{(j-1)}) - d_{\text{Fit}}^{(j)})^2$ 
14:    Estimate the gradient of the cost function:  $\frac{\partial C(P_E)}{\partial P_E}$ 
15:    Update the emitter location:
16:     $\mathbf{Y}_p^{(k)} := P_E^{(j)} \leftarrow P_E^{(j-1)} - \eta \frac{\partial C(P_E)}{\partial P_E}$ 
17:   end for
18:   Kalman gain and state update:
19:    $\mathbf{KG}^{(k)} = \bar{P}^{(k)} \mathbf{H}^T(k) [\mathbf{H}^{(k)} \bar{P}^{(k)} \mathbf{H}^T(k) + \mathbf{R}^{(k)}]^{-1}$ 
20:   Updated state:  $\mathbf{X}^{(k)} = \bar{\mathbf{X}}^{(k)} + \mathbf{KG}^{(k)} [\mathbf{Y}_p^{(k)} - \mathbf{H}\bar{\mathbf{X}}^{(k)}]$ 
21:   Updated covariance:  $\mathbf{P}^{(k)} = (\mathbf{I} - \mathbf{KG}^{(k)} \mathbf{H}^T) \bar{\mathbf{P}}^{(k)}$ 
22: end for
```

In Algorithm 1, K is the number of discrete steps (i.e., $K = 20$) along a linear trajectory at which incorrect depth measurements, $d^{(k)}$, are obtained and sequentially input to Algorithm 1, where $k = \{1, \dots, K\}$ is the number of incorrect depth measurements. The emitter position is updated iteratively for J gradient descent steps. $\mathbf{F} \in \mathbb{R}^{6 \times 6}$ is the state transition matrix that is defined as $\mathbf{F} = \begin{bmatrix} \mathbf{I}_{3 \times 3} & \mathbf{T}_s \mathbf{I}_{3 \times 3} \\ \mathbf{0}_{3 \times 3} & \mathbf{I}_{3 \times 3} \end{bmatrix}$, where \mathbf{T}_s

is the sampling interval. $\mathbf{X}^{(k)} \in \mathbb{R}^{6 \times 1}$ is the state vector that contains the 3D position of emitter and its 3D velocity. $\mathbf{P}^{(k)} \in \mathbb{R}^{6 \times 6}$ is the covariance matrix. Moreover, $\mathbf{W}^{(k)} \sim \mathcal{N}(0, \sigma_W^2)$, $\mathbf{R}^{(k)} \sim \mathcal{N}(0, \sigma_R^2)$, and $\mathbf{Q}^{(k)} \sim \mathcal{N}(0, \sigma_Q^2)$ denote the process, observation, and covariance noises. \mathbf{H} denotes the measurement matrix. In our setting, it is the identity matrix \mathbf{I} . \mathbf{KG} denotes the Kalman gain step 17. Step 5 and 6 propagate the predicted state that estimates the current state variables known as prior estimates and the associated covariance matrix. The update step 18 and 19 update the current state variables, known as posterior estimates. The emitter position measurements, \mathbf{Y}_p , are generated from the depth measurements and can be incorporated within the measurement model in step 18 for obtaining the predicted position (e.g., emitter position). By doing so, the KF tracks the correct position which is governed by pseudo-measurements, and is aware of the system dynamics.

For our validation of this method, we rely on realistic simulations of 3D target points in unknown source position settings. The initial guess for the proposed algorithm comes from the state of a probabilistic filter (i.e., the KF).

III. RESULTS AND DISCUSSION

In our computer experiments, local planarity is restricted to vertical planes. A number of numerical simulations are carried out to validate our novel algorithm over synthetically generated passive ToF data. We consider a single target, where the emitter, receiver, and target 3D points are defined to simulate a passive setup. In this context, we use the camera lens normals to obtain the target 3D plane points. To generate the incorrect depth, we employ the bistatic geometry (3) on 3D plane points to emulate real sensor measurements. The receiver is located at the origin of the coordinate system $P_R = (0, 0, 0)$ cm and the emitter is moving over a linear trajectory.

In this section, we validate our proposed algorithm via numerical simulations in 3D space. The linear trajectory is uniformly distributed in 20 samples, this is known as *incorrect depth measurements* d , with the step of 0.5 cm (i.e., 9.5-20 cm), corresponding to a linear speed of 250 cm/s and a frame rate of 5 FPS to attain the set of incorrect depth measurements. An initial guess for the first location is drawn from the 3D normal distribution $\mathcal{N}(P_E, \sigma_{P_E}^2)$ with $\sigma_{P_E}^2 \in \{2, 3, 10\}$ cm then the KF takes the role to provide a better initial value in the next step. The camera frame rate defines the time step of a filter, $T_s = 0.2$ s, i.e., 5 FPS. One example of obtained trajectories is demonstrated in Fig. 2(a), which shows the result of the estimation of source position and follows the linear trajectory. Thus, using KF is more relevant in tracking problems. Fig. 2(b) demonstrates the cost function and the emitter source position error. The first iteration is based on a random seed then KF keeps track of the emitter position. We demonstrate only three estimation measurements from the KF-driven algorithm, which yielded a value of the cost function of $50 \mu \text{ m}^2$, reaching machine precision, and an emitter position error of approximately 0.8 cm. Fig. 3 shows GT depth (left) and incorrect depth (middle) obtained from the bistatic computations and depth reconstruction of a vertical plane patch is shown on the right side.

We have pre-computed the measurement noise variance according to the expected error in the estimation of the pseudo-measurements. We obtained a minimum error of KF positioning in the sub-centimetric scale, approximately 0.8 cm, and an absolute estimated depth error of 0.15 cm is attained as shown in Fig. 4. Table 1 provides a comparison of the positioning error obtained (method in [12]) without KF and

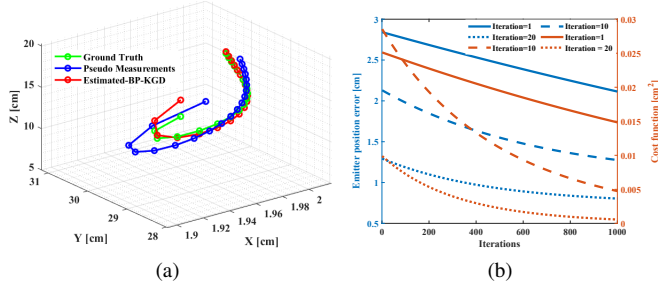


Fig. 2. (a) Source position estimation using blind source localization with KF and GD. (b) Source position error and value of the cost function with respect to iteration numbers for the pseudo-measurements estimation through gradient descent optimization.

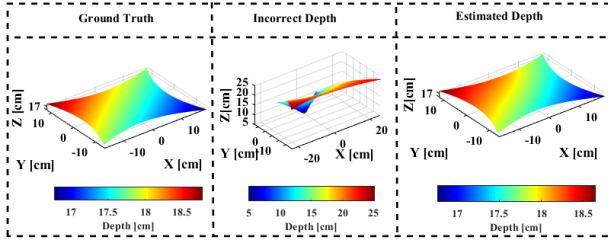


Fig. 3. Depth reconstruction based on estimated source position via blind source localization with KF and GD.

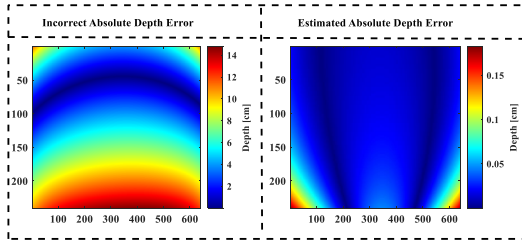


Fig. 4. Absolute depth reconstruction error based on estimated and incorrect depth using blind source localization.

with KF. The proposed method allows a reduction of the source location error between 77% and 85% with respect to the prior work.

TABLE 1. Performance analysis of source position and cost function.

Parameter	Worst [12]	Medium [12]	Best [12]	This work
Position error	5.5 cm	4 cm	3.5 cm	0.8 cm
Cost function	0.12 cm ²	0.41 mm ²	80 μ m ²	5.9 μ m ²

IV. CONCLUSION

In this letter, a novel algorithm is proposed to remove the initialization step arising in blind source localization for joint estimation of the 3D source position and retrieval of the correct depth in passive ToF imaging with an unknown emitter position. Adopting a blind source localization bistatic framework, the method includes a gradient descent optimization procedure between the propagation and update steps of a Kalman filter structure that keeps track of the source trajectory. Thanks to the KF, the proposed algorithm attains a better agreement between the GT and the estimated emitter position

when exploiting the local vertical planarity in the scene. Future lines of work will focus on exploring source localization in imperfect planes in an unknown environment or adverse conditions.

ACKNOWLEDGMENT

This project has received funding from the European Union's Horizon 2020 research and innovation programme under the Marie Skłodowska-Curie grant agreement No: 860370 (MENLAOS^{NT}).

REFERENCES

- [1] F. Ahmed, M. Heredia Conde, P. L. Martínez, T. Kerstein, and B. Buxbaum, "Pseudo-passive time-of-flight imaging: Simultaneous illumination, communication, and 3D sensing," *IEEE Sensors Journal*, vol. 22, no. 21, pp. 21218–21231, 2022.
- [2] I. B. F. De Almeida, M. Chafii, A. Nimr, and G. Fettweis, "Blind transmitter localization in wireless sensor networks: A deep learning approach," in *2021 IEEE 32nd Annual International Symposium on Personal, Indoor and Mobile Radio Communications (PIMRC)*, pp. 1241–1247, IEEE, 2021.
- [3] A. M. Abdalmalek, M. Mahmoud, A. E.-R. A. El-Fiky, H. A. Fayed, and M. H. Aly, "Improved indoor visible light positioning system using machine learning," *Optical and Quantum Electronics*, vol. 55, no. 3, p. 209, 2023.
- [4] S. C. Diamantas, A. Oikonomidis, and R. M. Crowder, "Depth estimation for autonomous robot navigation: A comparative approach," in *2010 IEEE International Conference on Imaging Systems and Techniques*, pp. 426–430, IEEE, 2010.
- [5] R. de Queiroz Mendes, E. G. Ribeiro, N. dos Santos Rosa, and V. Grassi Jr, "On deep learning techniques to boost monocular depth estimation for autonomous navigation," *Robotics and Autonomous Systems*, vol. 136, p. 103701, 2021.
- [6] X. Dong, M. A. Garratt, S. G. Anavatti, and H. A. Abbass, "Towards real-time monocular depth estimation for robotics: A survey," *IEEE Transactions on Intelligent Transportation Systems*, vol. 23, no. 10, pp. 16940–16961, 2022.
- [7] C. Ren and L. Liu, "Towards full passive internet of things: Symbiotic localization and ambient backscatter communication," *IEEE Internet of Things Journal*, pp. 1–1, 2023.
- [8] K. Wu, J. A. Zhang, and Y. J. Guo, *Joint communications and sensing: From fundamentals to advanced techniques*. John Wiley & Sons, 2022.
- [9] J. A. Zhang, F. Liu, C. Masouros, R. W. Heath, Z. Feng, L. Zheng, and A. Petropulu, "An overview of signal processing techniques for joint communication and radar sensing," *IEEE Journal of Selected Topics in Signal Processing*, vol. 15, no. 6, pp. 1295–1315, 2021.
- [10] H. Elgala, R. Mesleh, and H. Haas, "Indoor optical wireless communication: potential and state-of-the-art," *IEEE Communications Magazine*, vol. 49, no. 9, pp. 56–62, 2011.
- [11] L. Rui and K. Ho, "Elliptic localization: Performance study and optimum receiver placement," *IEEE Transactions on Signal Processing*, vol. 62, no. 18, pp. 4673–4688, 2014.
- [12] F. Ahmed, M. Heredia Conde, and P. López Martínez, "GIPS: Geometry-inspired passive ToF sensing for 3D depth reconstruction," in *2023 31st European Signal Processing Conference (EUSIPCO)*, 2023.
- [13] J. Boger-Lombard and O. Katz, "Passive optical time-of-flight for non line-of-sight localization," *Nature communications*, vol. 10, no. 1, p. 3343, 2019.
- [14] E. L. Francois, J. Herrnsdorf, J. J. D. McKendry, L. Broadbent, G. Wright, M. D. Dawson, and M. J. Strain, "Synchronization-free top-down illumination photometric stereo imaging using light-emitting diodes and a mobile device," *Opt. Express*, vol. 29, pp. 1502–1515, Jan 2021.
- [15] F. Wagner, F. Schiffrers, F. Willomitzer, O. Cossairt, and A. Velten, "Intensity interferometry-based 3D imaging," *Optics Express*, vol. 29, no. 4, pp. 4733–4745, 2021.
- [16] E. Delage, H. Lee, and A. Y. Ng, "Automatic single-image 3D reconstructions of indoor Manhattan world scenes," in *Robotics Research: Results of the 12th International Symposium ISRR*, pp. 305–321, Springer, 2007.
- [17] A. Bhandari, M. Heredia Conde, and O. Löffel, "One-bit time-resolved imaging," *IEEE Transactions on Pattern Analysis and Machine Intelligence*, vol. 42, no. 7, pp. 1630–1641, 2020.
- [18] R. E. Kalman, "A new approach to linear filtering and prediction problems," 1960.
- [19] K. Kumar, R. K. Tiwari, S. Bhaumik, and P. Date, "Polynomial chaos Kalman filter for target tracking applications," *IET Radar, Sonar & Navigation*, vol. 17, no. 2, pp. 247–260, 2023.
- [20] S. Mahfouz, F. Mourad-Chehade, P. Honeine, J. Farah, and H. Snoussi, "Target tracking using machine learning and Kalman filter in wireless sensor networks," *IEEE Sensors Journal*, vol. 14, no. 10, pp. 3715–3725, 2014.